

High-Performance Aqueous/Organic Dye-Sensitized Solar Cells Based on Sensitizers Containing Triethylene Oxide Methyl Ether

Ryan Yeh-Yung Lin,^[a] Feng-Ling Wu,^[a] Chun-Ting Li,^[b] Pei-Yu Chen,^[b] Kuo-Chuan Ho,^{*,[b, c]} and Jiann T. Lin^{*,[a]}

Metal-free dyes (EO1 to EO4) containing the hydrophilic triethylene oxide methyl ether (TEOME) unit in the spacer have been synthesized and used in dye-sensitized solar cells (DSSCs). Efficient lithium-ion trapping by TEOME results in improved open-circuit voltage (V_{OC}), leading to excellent conversion efficiency of the cells, ranging from 9.02 to 9.98% with I^-/I_3^- electrolyte

in acetonitrile under AM 1.5 illumination. The TEOME unit also enhances the wettability of the dye molecules for application in aqueous-based DSSCs. Aqueous-based DSSCs with a dual TEMPO/iodide electrolyte exhibit high V_{OC} values (0.80–0.88 V) and very promising cell performances of up to 5.97%.

Introduction

Dye-sensitized solar cells (DSSCs) have been deemed as promising low-cost, sustainable power sources. An impressively high efficiency of 13% has been achieved with a DSSC based on a porphyrin sensitizer and cobalt redox mediator under AM 1.5 solar irradiation.^[1a] In comparison, high power conversion efficiencies of 11.50 and 12.5% were reported for DSSCs based on a polypyridyl ruthenium(II) complex with an I^-/I_3^- redox mediator^[1b] and a metal-free organic sensitizer with a cobalt redox mediator,^[1c] respectively. Metal-free organic dyes have attracted increasing attention due to their high molar extinction coefficients, low cost, and flexibility in the molecular design. Among them, phenothiazine-based sensitizers are interesting for the following reasons: 1) the phenothiazine entity is proven to be an effective electron-donating entity, and 2) the nonplanar nature of the phenothiazine entity is beneficial at impeding molecular aggregation and the formation of intermolecular excimers.^[2a] Several phenothiazine-based sensitizers have also been successfully used for high-performance DSSCs.^[2b–e] In 2013, the group of Wong reported a series of phenothiazine-based sensitizers for high cell performance DSSCs,^[2f] and the highest power conversion efficiency of 8.18% even surpassed

that of N719 (7.73%) under one sun conditions. In 2015, the group of Lin also reported phenothiazine-based sensitizers that possessed double anchors, and the best efficiency exceeded that of the N719-based cell by about 13%.^[2g] We therefore further exploited phenothiazine dyes for high-performance DSSCs.

Earlier we developed a water-soluble dual-redox couple, which consisted of imidazolium iodide and 2,2,6,6-tetramethylpiperidin-*N*-oxyl (TEMPO) units; this could increase the open-circuit voltage (V_{OC}) of the DSSC due to blocking of the disproportionation of the iodine radical anion.^[3] Therefore, aqueous DSSCs were also tested with the phenothiazine dyes newly developed by us for DSSCs together with the dual-redox couple, and an intriguingly high conversion (4.96%) was achieved.^[4a] Compared with organic solvents, water is abundant, inexpensive, and environmentally benign. To date, several aqueous DSSCs with efficiencies higher than 3% have been reported,^[4a–h] and a record cell efficiency of 5.64% was reported by Spiccia et al. based on a metal-free dye after surface treatment with octadecyltrichlorosilane for dark-current suppression.^[4e] Although water is believed to lead to dye leaching,^[5a] loss of iodine,^[5b,c] and band edge movement,^[5d] there has been one report on good cell stability with water added to the cells.^[5e] There was also an attempt to improve the dye stability towards leaching in water by replacing the common anchor, a cyanoacrylate moiety, with a more robust hydroxamic acid anchor.^[5f]

Because most organic dyes are hydrophobic, incomplete wetting of the aqueous electrolyte/dye-coated TiO_2 film surface may hamper ion diffusion and slow down dye regeneration. Therefore, nonionic (such as Triton-X100,^[4b] Tween-20,^[4c] and polyethylene glycol^[5d]) and ionic surfactants^[5g] (such as hexadecyltrimethylammonium bromide and triethylammonium perfluorooctane sulfonate) were added to water to improve the interfacial contact between the aqueous electrolyte and

[a] Dr. R. Y.-Y. Lin,⁺ F.-L. Wu,⁺ Prof. J. T. Lin
Institute of Chemistry, Academia Sinica
Nankang 11529, Taipei (Taiwan)ca.edu.tw
E-mail: jtlin@gate.sinica.edu.tw

[b] C.-T. Li, P.-Y. Chen, Prof. K.-C. Ho
Department of Chemical Engineering
National Taiwan University
Taipei 10617 (Taiwan)
E-mail: kcho@ntu.edu.tw

[c] Prof. K.-C. Ho
Institute of Polymer Science and Engineering
National Taiwan University, Taipei 10617 (Taiwan)

[⁺] These authors contributed equally to this work.

Supporting Information for this article is available on the WWW under <http://dx.doi.org/10.1002/cssc.201500589>.

dye-coated TiO₂ film. Alternatively, a transparent TiO₂ layer was added to the dye-coated photoelectrode by atomic layer deposition to enhance photoelectrode wettability.^[5h] Upon observing that oligo(ethylene oxide) was water compatible, we decided to develop phenothiazine-based dyes containing triethylene oxide methyl ether (TEOME) units for application as sensitizers for aqueous DSSCs. To the best of our knowledge, there have been few reports on dye molecules with the aim of ameliorating water compatibility for aqueous-based DSSCs.^[4f,g] A systematic investigation into wettability improvement through structural modification to dyes is also needed for the advancement of the field. We were also aware that the TEOME entity incorporated in the bipyridyl ligand of ruthenium complexes helped with trapping of the lithium ion and resulted in higher V_{OC} values of the cells.^[6] Therefore, TEOME-containing phenothiazine sensitizers also offer an opportunity to boost the cell performance of DSSCs with organic solvents.

Results and Discussion

Synthesis of the materials

Figure 1 shows the structures of new organic sensitizers and a known sensitizer (S1)^[2f] without TEOME as the reference. The main synthetic pathways are depicted in Scheme 1. The TEOME entity can be introduced into the molecule at the nitrogen atom of the phenothiazine core through a [Pd(dba)₂]-catalyzed C–N coupling reaction^[7a,b] of 10*H*-phenothiazine with 1-bromo-4-[[2-(2-methoxyethoxy)ethyl]peroxy]benzene (such as 1). Alternatively, it can be tethered to the molecule through the C-3 (or C-7) substituent of the phenothiazine by a palladium-catalyzed Suzuki–Miyaura coupling reaction^[7c] of TEOME-substituted phenyl bromide and dioxaborolyl phenothiazine, or palladium-catalyzed Stille coupling reaction^[7d] of TEOME-substituted phenyl stannane and phenothiazinyl bromide. The formyl group was introduced through a Vilsmeier–Haack reaction either before or after the catalyzed C–C coupling reaction. The last step toward the desired products, EO1–EO5, was Knoevenagel condensation of the appropriate aldehyde with cyanoacetic acid. It is worth noting that Suzuki–Miyaura in-

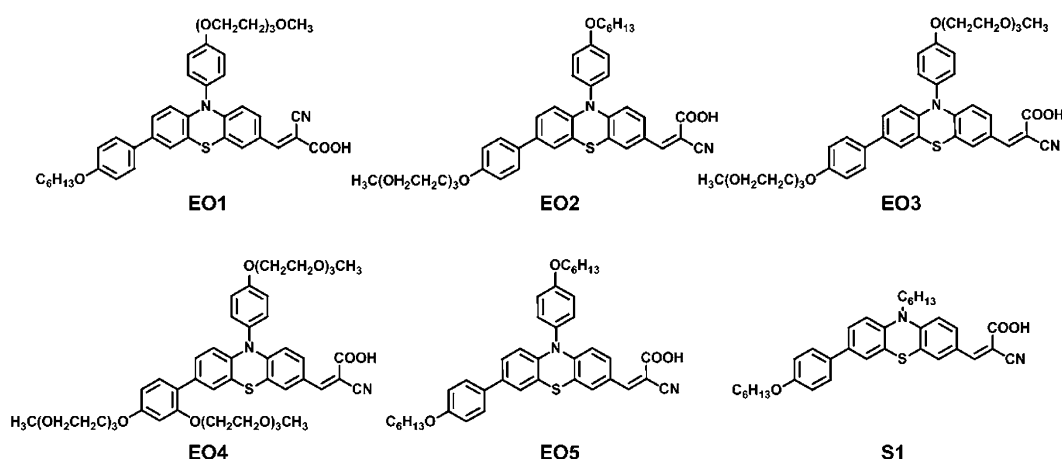
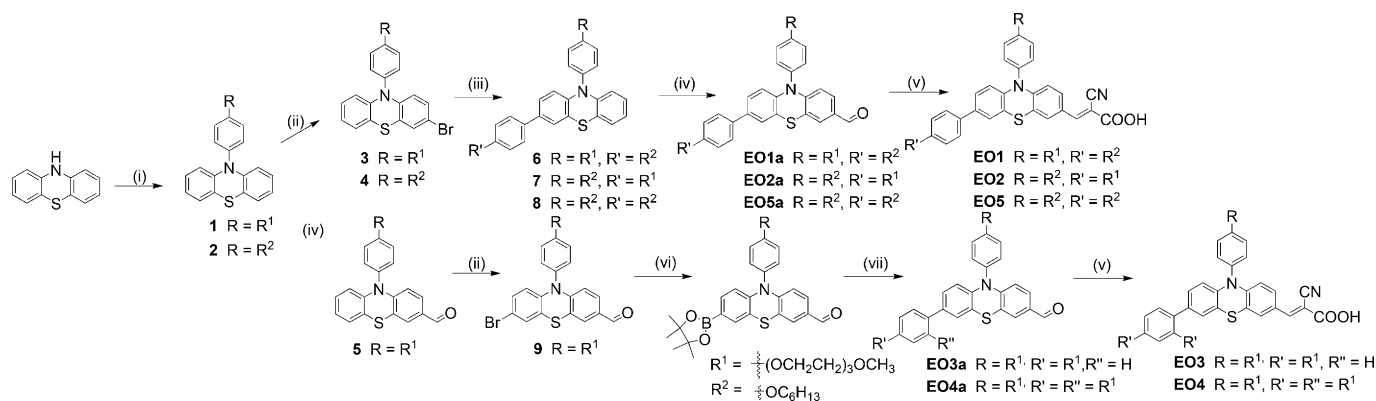


Figure 1. Structure of the dyes described herein.



Scheme 1. Synthetic pathways for the EO dyes. (i) 1-bromo-4-(hexyloxy)benzene, [Pd(dba)₂] (dba = dibenzylideneacetone), Pt(Bu)₂, NaOtBu, toluene, 120 °C, 20 h; (ii) *N*-bromosuccinimide (NBS), CH₂Cl₂, 18 h; (iii) [Pd(PPh₃)₂Cl₂], tributyl[4-(hexyloxy)phenyl]stannane, 90 °C, 20 h; (iv) POCl₃, DMF, 60 °C, 18 h; (v) cyanoacetic acid, NH₄OAc, AcOH, 120 °C; (vi) bis(pinacolato)diboron, KOAc, [PdCl₂(dppf)] (dppf = 1,1'-bis(diphenylphosphino)ferrocene), 1,4-dioxane, 120 °C, 20 h; (vii) [Pd(PPh₃)₄], 2 M K₂CO₃, 1-bromo-2,4-bis[2-(2-(2-methoxyethoxy)ethoxy)ethoxy]benzene, toluene, 120 °C, 20 h.

stead of Stille coupling has to be used for the phenyl bromide with two TEOME substituents.

Optical properties

The electronic absorption spectra of the EO dyes in THF have two major bands in the range of $\lambda = 300\text{--}500\text{ nm}$ (Figure 2a).

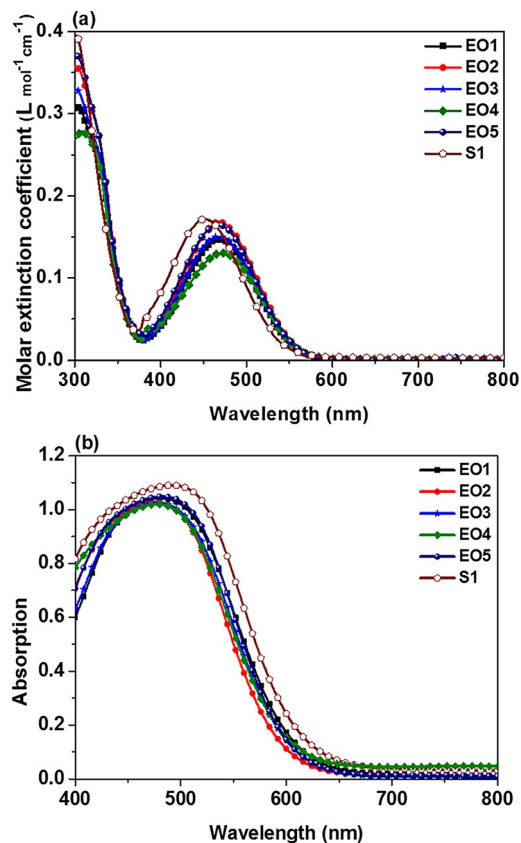


Figure 2. (a) Absorption spectra of the dyes in THF. (b) Absorption spectra of the EO dyes on a thin film of TiO₂.

The band at $\lambda_{\text{abs}} < 400\text{ nm}$ is attributed to the $\pi\text{--}\pi^*$ transition, and that in the longer wavelength region ($\lambda = 380\text{--}600\text{ nm}$) is ascribed to the intramolecular charge-transfer (ICT) transition with $\pi\text{--}\pi^*$ transition character. The λ_{abs} value of EO5 ($\lambda = 470\text{ nm}$) is larger than that of S1 ($\lambda = 452\text{ nm}$). Compared with the hexyl group, the better electron-donating 4-hexoxyphenyl group at the nitrogen atom of the phenothiazine entity clearly more efficiently enhances the donating power of the phenothiazine entity.

Although EO4 has two TEOME substituents, there is only a marginal change in the λ_{abs} values ($< 6\text{ nm}$) compared with those of other dyes. It is possible that the TEOME substituent at the *ortho* position of the phenyl ring results in a larger twist angle between the TEOME-containing phenyl ring and the phenothiazine entity. The absorption spectra (Figure 2b) of the dyes adsorbed on TiO₂ extend beyond $\lambda = 650\text{ nm}$, which indicates J aggregation of the dyes.

Electrochemical properties

Relevant electrochemical data obtained from cyclic voltammetry are presented in Table 1 and the spectra are shown in Figure S1 in the Supporting Information. The first reversible wave is attributed to the oxidation of phenothiazine and decreases in the order of EO1 \approx EO2 \approx EO3 \approx EO5 $>$ EO4. The presence of an extra electron-donating TEOME at the *ortho* position of the phenyl ring significantly increases the electron density of phenothiazine in EO4. The excited-state potential (E_{0-0}^* , -1.17 to -1.22 V vs. NHE), estimated from the difference (E_{0-0}^* of the first oxidation potential at the ground state and the zero-zero excitation energy (E_{0-0}) of the EO sensitizers, is more negative than the conduction band edge of the TiO₂ electrode (-0.5 V vs. NHE), which ensures enough driving force for electron injection into the conduction band of TiO₂.

Photovoltaic devices

The photovoltaic performance statistics of DSSCs with the iodide electrolyte in CH₃CN under AM 1.5G illumination are collected in Table 2. The photocurrent–voltage ($J\text{--}V$) curves and IPCE spectra of the cells are plotted in Figure 3a and b, respectively. The cell efficiencies of the EO dyes (8.18 to 9.98%) are higher than that of S1 (8.02%), and EO3 has the best performance of all. For a fair comparison, the dye-loading densities on the photoanode were also measured (see Table 2). The slightly lower J_{SC} value of EO1 may be partially attributed to its lower dye loading. Charge extraction measurements (see below) indicate a downward shift of the TiO₂ conduction band edge for the DSSCs of EO5 and S1. It is possible that there are fewer lithium cations adsorbed on the TiO₂ surface due to trapping by TEOME, which leads to a lower conduction band edge of TiO₂. All other EO dyes have comparable TiO₂ conduction band edges, which implies that one TEOME chain is sufficient to trap the lithium cations in solution. The photocurrents estimated from integrating the product of the IPCE value at each wavelength and the photon flux density data in the AM 1.5 solar spectrum (100 mW cm^{-2}) were about 12.9, 13.9, 15.5, 15.4, 12.6, and 13.1 mA cm⁻² for the EO1–EO5 and S1 cells, respectively. The results are smaller than the experimental value.

Table 1. Electro-optical parameters of the dyes.

Dye	λ_{abs} [nm] ($\epsilon \times 10^{-4}\text{ L mol}^{-1}\text{ cm}^{-1}$) ^[a]	λ_{em} ^[a] [nm]	$E_{1/2(\text{ox})}$ ^[b] [mV]	HOMO/LUMO [eV]	E_{0-0} ^[c] [eV]	E_{0-0}^* ^[d] [V]
EO1	468 (1.48)	614	378	5.48/3.21	2.27	-1.19
EO2	467 (1.68)	616	378	5.48/3.23	2.25	-1.17
EO3	469 (1.51)	614	378	5.48/3.23	2.25	-1.17
EO4	472 (1.30)	615	352	5.45/3.21	2.24	-1.19
EO5	470 (1.65)	613	378	5.48/3.18	2.30	-1.22

[a] Recorded in THF at 298 K. [b] Recorded in THF. $E_{\text{ox}} = 1/2(E_{\text{pa}} + E_{\text{pc}})$, $\Delta E_{\text{p}} = E_{\text{pa}} - E_{\text{pc}}$, in which E_{pa} and E_{pc} are the anodic and cathodic peak potentials, respectively. The oxidation potential reported is adjusted to the potential of ferrocene, which was used as an internal reference. The values in parentheses are the peak separation of the cathodic and anodic waves. Scan rate: 100 mV s^{-1} . [c] The band gap, E_{0-0} , was derived from the intersection of the absorption and emission spectra. [d] E_{0-0}^* : The excited-state oxidation potential versus a normal hydrogen electrode (NHE).

Dye	V_{OC} [V]	J_{SC} [mA cm^{-2}]	FF	η [%]	$J_{SC-IPCE}$ [mA cm^{-2}]	Dye loading [mol cm^{-2}]	θ_c [°]
EO1	0.77 ± 0.004	15.65 ± 0.342	0.68 ± 0.003	8.22 ± 0.190	12.9	5.18×10^{-7}	103.00
EO2	0.80 ± 0.005	16.50 ± 0.055	0.68 ± 0.007	9.02 ± 0.028	13.9	5.56×10^{-7}	95.14
EO3	0.82 ± 0.003	17.81 ± 0.101	0.68 ± 0.003	9.98 ± 0.047	15.5	5.67×10^{-7}	37.39
EO4	0.81 ± 0.004	17.67 ± 0.150	0.68 ± 0.004	9.79 ± 0.031	15.4	6.03×10^{-7}	15.94
EO5	0.77 ± 0.008	15.70 ± 0.077	0.68 ± 0.004	8.18 ± 0.058	12.6	5.48×10^{-7}	117.36
S1	0.76 ± 0.005	16.12 ± 0.062	0.66 ± 0.006	8.02 ± 0.091	13.1	5.90×10^{-7}	115.63
N719	0.72	18.41	0.65	8.61			

[a] Experiments were conducted by using TiO_2 photoelectrodes approximately $12 \mu\text{m}$ thick with a 0.16 cm^2 working area on fluorine-doped tin oxide (FTO; $15 \Omega/\text{sq}$) substrates. Each result was obtained from three DSSCs. J_{SC} is the short-circuit current, FF is the fill factor, IPCE is the incident photon-to-current conversion efficiency, and θ_c is the contact angle.

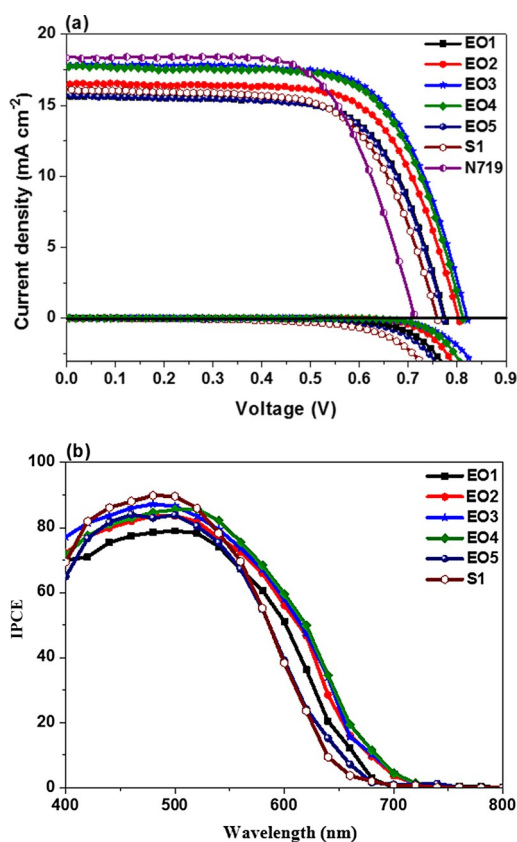


Figure 3. (a) J - V curves and (b) IPCE spectra of DSSCs based on the dyes reported herein.

This discrepancy may be attributed to the filtration of IR radiation by a water filter in our light source during measurements, whereas the real sun spectrum covers the near-IR region.^[8] The dark current (Figure 3a) of the cells decreases in the order of $S1 > EO5 > EO1 > EO2 > EO4 > EO3$. As expected, more effective dark-current suppression for the cells of EO2, EO3, and EO4 significantly improved the V_{OC} values in these cells. The larger dark currents in S1 and EO5 clearly indicate that the TEOME entity helps with dark-current suppression similar to a long alkyl chain. TEOME connected to the phenothiazine through

the C7 carbon (code symbol: C-PhTEOME) seems to be more effective in dark-current (Figure 3a) suppression than that through nitrogen (code symbol: N-PhTEOME), as evidenced from electrochemical impedance spectroscopy (EIS) and intensity-modulated photovoltage spectroscopy (IMVS; see below) data for EO1 and EO2.

Dye S1 on TiO_2 has the most redshifted spectrum compared with the EO dyes, which is consistent with its dye aggregation upon adsorption.^[21] Consequently,

the most blueshifted IPCE spectrum and lower short-circuit current of the S1-based DSSC can be partly attributed to aggregation-induced quenching of the dye excited state. Although less severe than that of S1, dye aggregation of EO5 (Figure 2b) also jeopardizes electron injection and results in the cutoff of the IPCE spectra (Figure 3b) at a shorter wavelength, leading to lower short-circuit currents. The EIS data of DSSCs in the dark are shown in Figure S2 in the Supporting Information. The intermediate frequency semicircle in the Nyquist plot provides information on charge transfer between the TiO_2 surface and the electrolyte, that is, the dark current. Resistance towards the dark current decreases in the order of $EO3 > EO4 > EO2 > EO1 > EO5 > S1$, which is consistent with the dark current (Figure 3a) and observed V_{OC} values (Table 2).

The V_{OC} value is determined by the position of the conduction band (E_{CB}) edge and electron density in the TiO_2 film.^[9] The relative conduction band shift of TiO_2 was estimated by means of the charge extraction method (CEM), as shown in Figure 4a. The cell of S1 has the highest d_n (electron density) value of all at the same V_{OC} , which indicates that it has the most downshifted conduction band edge of TiO_2 . The cell of EO5 has the second highest d_n , and therefore, also a downshifted conduction band edge of TiO_2 . All other EO dyes have comparable conduction band edges of TiO_2 . The electron lifetime (τ) was derived as a function of V_{OC} by measuring the IMVS, as shown in Figure 4b. The trend is also consistent with the V_{OC} and EIS data in the dark (see above). At the same voltage, the DSSCs of EO5 and S1 have shorter lifetimes than the other DSSCs. This further substantiates the importance of TEOME in dark-current suppression.

DSSCs with the JC-IL aqueous-based electrolyte

In addition to dye stability, electrolyte diffusion and dye wettability are also important for aqueous-based DSSCs. In this study, we deliberately incorporated the TMEOM entity at the dye molecule to improve the wettability of the dye molecule to facilitate interfacial electron transfer between the hydrophilic electrolyte and the hydrophobic dye molecule, that is, dye regeneration. Contact angle analysis was used to investigate the hydrophilic/-phobic properties of the EO and S1 sensitizers.

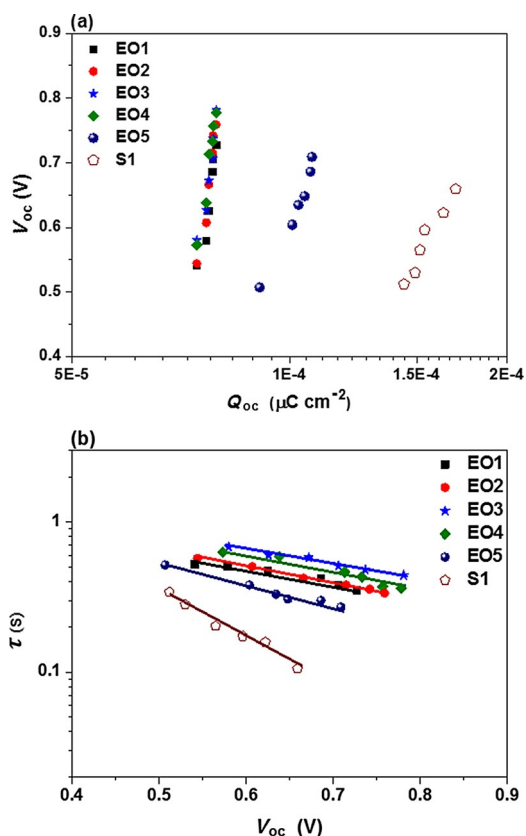


Figure 4. (a) V_{OC} as a function of electron density for DSSCs sensitized with EO dyes. (b) Electron lifetime as a function of V_{OC} for DSSCs sensitized with EO dyes.

The contact angles of a deionized water drop on the surface of the EO and S1 sensitizers are shown in Figure 5 and the data are compiled in Table 2. The dyes without TEOME, EO5 and S1,

have contact angles of over 115° . As the number of TEOME unit increases, the contact angle decreases: EO1, 103.00° ; EO2, 95.14° ; EO3, 37.39° ; EO4, 15.94° . It appears that EO1–EO4 have higher wettability than that of EO5 and S1. The J – V curves and IPCE spectra of the DSSCs with water-based JC-IL (1-butyl-3- $\{2$ -oxo-2- $\{2,2,6,6$ -tetramethylpiperidin-1-oxyl-4-yl)amino]ethyl}-1*H*-imidazol-3-ium iodide) electrolyte^[4a] measured under AM 1.5G illumination are shown in Figure 6a and b, respectively, and the corresponding photovoltaic parameters are given in Table 3. The cells of EO1–EO4 exhibited excellent cell performances compared with those of EO5 and S1, which suggested that the dye with higher wettability had a better cell performance. Hupp et al. found that enhanced photoelectrode wettability through post-assembly atomic layer deposition of additional TiO_2 also led to better cell performance.^[5h] We speculate that higher wettability of the dye increases interfacial electron transfer between the electrolyte and oxidized dye molecule. However, there is slight discrepancy between EO4 and EO3. In addition to the wettability, the access of the elec-

Table 3. Photovoltaic parameters of the DSSCs with JC-IL water-based electrolytes.^[a]

Dye	V_{OC} [V]	J_{SC} [mA cm^{-2}]	FF	η [%]
EO1	0.84	7.11	0.68	4.04
EO2	0.85	8.31	0.67	4.73
EO3	0.88	9.87	0.68	5.97
EO4	0.86	8.63	0.67	4.98
EO5	0.84	5.97	0.65	3.27
S1	0.81	5.76	0.66	3.11

[a] Experiments were conducted by using TiO_2 photoelectrodes approximately $10 \mu\text{m}$ thick with a 0.16 cm^2 working area on FTO ($15 \Omega/\text{sq}$) substrates.

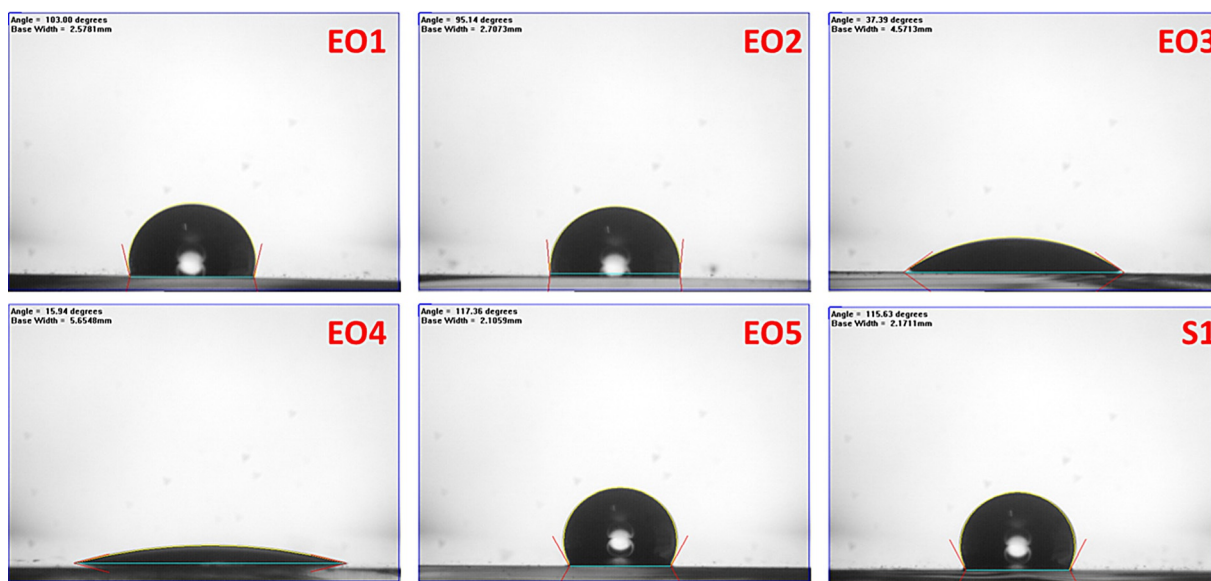


Figure 5. Cross-sections of working electrodes with EO sensitizers and a drop of deionized water positioned on the top of the cell; this was used to estimate θ_c [°].

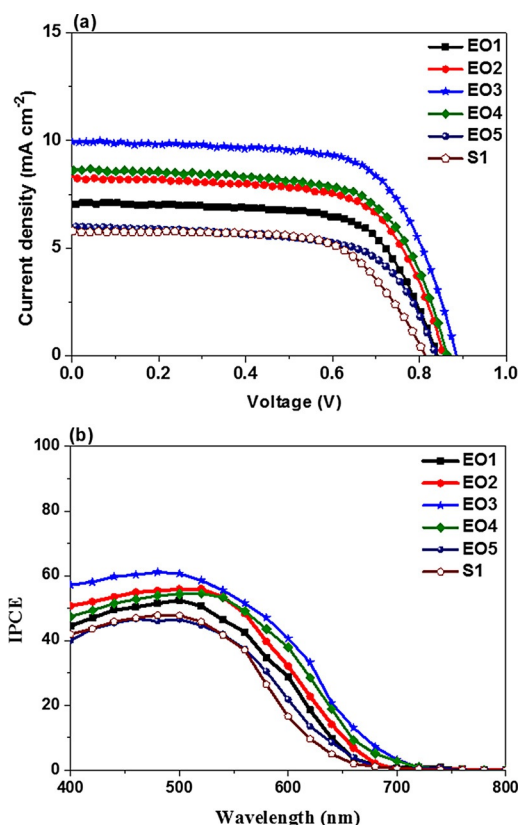


Figure 6. (a) *J*-*V* curves with the JC-IL water-based electrolyte. (b) IPCE spectra of DSSCs based on the dyes reported herein with the JC-IL water-based electrolyte.

trolyte towards the sensitizer for electron transfer is also likely to be affected by the geometry of the dye molecule. Therefore, further studies are needed to elucidate the detailed mechanism involved. Sensitizer EO3 has the best cell performance (η : 5.97%; V_{OC} : 0.88 V; J_{SC} : 9.87 mA cm⁻²; FF: 0.68) and slightly outperformed that in a previous report (η : 5.64%; V_{OC} : 0.821 V; J_{SC} : 10.17 mA cm⁻²; FF: 0.68).^[5e] It is noteworthy that, without surface treatment with octadecyltrichlorosilane, the efficiency of the cell with EO3 drops to 4.09%. Compared with DSSCs with I⁻/I₃⁻ and CH₃CN-based electrolytes, EO-sensitized DSSCs with JC-IL electrolyte have remarkably higher V_{OC} values, but significantly lower J_{SC} values. Similar to our previous observations, the lower J_{SC} values of the water-based electrolyte may be attributed to the poor diffusion rate in H₂O,^[4a] and the higher V_{OC} values stem from the more positive redox potential of N-O[•]/N=O⁺ of the redox mediator due to the successful interception of I₂^{-•} by the N-O radical.^[10]

Conclusions

Incorporation of the TEOME entity into phenothiazine-based metal-free organic sensitizers was beneficial at increasing the wettability of the dyes and stronger trapping of lithium ions in the electrolytes. They were successfully applied for high-performance organic-solvent- and water-based DSSCs. Because TEOME helped with lithium-ion trapping and dark-current sup-

pression, DSSCs based on an organic solvent exhibited excellent efficiencies (8.18–9.98%) with the standard I⁻/I₃⁻ electrolyte under AM 1.5 illumination. The best cell performance was higher than that of the N719-based standard cell by about 14%. Water-based DSSCs with the JC-IL dual-redox couple had V_{OC} values exceeding 0.80 V, which was at least 50 mV higher than that of DSSCs with standard iodide electrolyte. The better wettability of the dyes (EO1–EO4) with TEOME led to better cell efficiencies, and the best efficiency surpassed the highest value reported to date.

Experimental Section

Materials and instrumentation

The solvents used were purified by standard procedures, or purged with nitrogen before use. ¹H and ¹³C NMR spectra were recorded on Bruker AV-400 and AMX-400 spectrometers. Electronic absorption spectra were measured on a Dynamica DB-20 UV/Vis spectrophotometer. Mass spectra (FAB) were recorded on a VG70-250S mass spectrometer. Elemental analyses were carried out on a PerkinElmer 2400 CHN analyzer. Chromatographic separations were conducted on silica gel (60M, 230–400 mesh).

Fabrication of DSSCs

The TiO₂ films used were comprised of a transparent layer and a scattering layer with thicknesses of 9 and 3 μm, respectively, as measured by means of a profilometer (Dektak3, Veeco/Sloan Instruments Inc., USA). The TiO₂ electrodes with a 0.16 cm² geometric area were immersed in a solution containing 3 × 10⁻⁴ M organic sensitizers in THF or in a solution containing 3 × 10⁻⁴ M of N719 (Solaronix S.A., Switzerland) in acetonitrile/*tert*-butanol (1:1 v/v) for 16 h. Platinized FTO was used as a counter electrode and was controlled to have an active area of 0.16 cm² by adhered polyester tape with a thickness of 60 μm. The JC-IL electrolyte contained 0.4 M JC-IL and 0.4 M NOBF₄ in water; and the iodide electrolyte contained 0.1 M LiI, 0.05 M I₂, 0.6 M 1,2-dimethyl-3-propylimidazolium iodide (DMPII), and 0.1 M guanidine thiocyanate (GuSCN) dissolved in a mixture of CH₃CN)/3-methoxypropionitrile (MPN; 1:1 v/v). A 0.4 × 0.4 cm² cardboard mask was clipped onto the device to constrain the illumination area. Photoelectrochemical characterizations of the solar cells were carried out by using an Oriel Class A solar simulator (Oriel 91195 A, Newport Corp.).

Characterization of DSSCs

Photocurrent–voltage characteristics of the DSSCs were recorded with a potentiostat/galvanostat (CHI650B, CH Instruments, Inc., USA) at a light intensity of 1.0 sun calibrated by an Oriel reference solar cell (Oriel 91150, Newport Corp.). The IPCE curves were obtained under short-circuit conditions. The light source was a class A quality solar simulator (PEC-L11, AM 1.5G, Peccell Technologies, Inc.); light was focused through a monochromator (Oriel Instrument, model 74100) onto the photovoltaic cell and measured with an optical detector (Oriel Instrument, model 71580) and power meter (Oriel Instrument, model 70310). The IMVS measurements were carried out on an electrochemical workstation (Zahner, Zennium) with a frequency response analyzer under white light-emitting diode (LED) illumination. The modulated light intensity was 10% or less than the base light intensity. The frequency range was set from 1 kHz to 0.1 Hz.

10-(4-{2-[2-(2-Methoxyethoxy)ethoxy]ethoxy}phenyl)-10H-phenothiazine (1)

10H-Phenothiazine (2.00 g, 10.0 mmol), 1-bromo-4-{2-[2-(2-methoxyethoxy)ethoxy]ethoxy}benzene (2.00 g, 6.27 mmol), sodium *tert*-butoxide (1.45 g, 15.1 mmol), and [Pd(dba)₂] (0.12 g) were added to a 100 mL two-necked round-bottomed flask under nitrogen. Dry toluene (15 mL) and tri(*tert*-butyl)phosphine (0.494 M in toluene, 1.0 mL) were injected into the flask and the solution was heated at 120 °C for 20 h. After the reaction was complete, the solution was extracted with CH₂Cl₂ and washed with brine. The organic extracts collected were dried over MgSO₄ and filtered. The filtrate was dried under vacuum, and the crude product was further purified by column chromatography by using CH₂Cl₂/ethyl acetate (EA; 20:1 v/v) as the eluent. The product was obtained as a brown oil (1.6 g, 65%). ¹H NMR (CDCl₃, 400 MHz): δ = 7.27 (d, 2H, *J* = 8.8 Hz), 7.10 (d, 2H, *J* = 8.8 Hz), 6.96 (dd, 2H, *J* = 7.2, 1.6 Hz), 6.82–6.73 (m, 4H), 6.16 (d, 2H, *J* = 8.8 Hz), 4.19 (t, 2H, *J* = 4.8 Hz), 3.90 (t, 2H, *J* = 4.8 Hz), 3.76 (m, 2H), 3.68 (m, 4H), 3.55 (m, 2H), 3.37 ppm (s, 3H).

10-[4-(Hexyloxy)phenyl]-10H-phenothiazine (2)

10H-Phenothiazine (1.55 g, 7.78 mmol), 1-bromo-4-(hexyloxy)benzene (2.00 g, 7.78 mmol), sodium *tert*-butoxide (1.12 g, 11.7 mmol), and [Pd(dba)₂] (0.13 g) were added to a 100 mL two-necked round-bottomed flask under nitrogen. Dry toluene (15 mL) and tri(*tert*-butyl)phosphine (0.494 M in toluene, 0.6 mL) were injected into the flask. The mixture was heated at 120 °C for 20 h. After the reaction was complete, the solution was extracted with CH₂Cl₂ and washed with brine. The organic extracts collected were dried over MgSO₄ and filtered. The filtrate was dried under vacuum and the crude product was further purified by column chromatography with hexanes/CH₂Cl₂ (6:1 v/v) as the eluent. The product was obtained as a white solid (2.5 g, 87%). ¹H NMR (CDCl₃, 500 MHz): δ = 7.27 (d, 2H, *J* = 8.5 Hz), 7.07 (d, 2H, *J* = 8.5 Hz), 6.96 (d, 2H, *J* = 7.5 Hz), 6.82–6.74 (m, 4H), 6.18 (d, 2H, *J* = 8.0 Hz), 4.01 (t, 2H, *J* = 6.0 Hz), 1.84–1.79 (m, 2H), 1.49–1.47 (m, 2H), 1.36 (m, 4H), 0.91 ppm (t, 3H, *J* = 5.0 Hz).

3-Bromo-10-(4-{2-[2-(2-methoxyethoxy)ethoxy]ethoxy}phenyl)-10H-phenothiazine (3)

Compound **1** was dissolved in CH₂Cl₂ (1.5 mL) in a round-bottomed flask and a solution of NBS (0.63 g, 3.54 mmol) in CH₂Cl₂ (1.5 mL) was added to the reaction mixture. The mixture was stirred for 18 h at room temperature and then poured into ice water, and extracted with CH₂Cl₂. The combined organic layers were dried over MgSO₄ and evaporated to dryness. The crude product was further purified by column chromatography on silica gel with CH₂Cl₂/EA (20:1 v/v) as the eluent. The product was obtained as a brown oil (1 g, 56%). ¹H NMR (CDCl₃, 400 MHz): δ = 7.23 (d, 2H, *J* = 8.4 Hz), 7.09 (d, 2H, *J* = 8.8 Hz), 7.06 (d, 1H, *J* = 2.0 Hz), 6.93 (dd, 1H, *J* = 7.2, 1.6 Hz), 6.87 (dd, 1H, *J* = 7.2, 1.6 Hz), 6.81–6.76 (m, 2H), 6.14 (dd, 1H, *J* = 7.6, 0.8 Hz), 5.99 (d, 1H, *J* = 8.8 Hz), 4.18 (t, 2H, *J* = 4.8 Hz), 3.89 (t, 2H, *J* = 4.8 Hz), 3.76–3.74 (m, 2H), 3.70–3.64 (m, 4H), 3.56–3.53 (m, 2H), 3.37 ppm (s, 3H).

3-Bromo-10-[4-(hexyloxy)phenyl]-10H-phenothiazine (4)

Compound **2** was dissolved in CH₂Cl₂ (4.0 mL) in a round-bottomed flask and a solution of NBS (0.90 g, 5.31 mmol) in CH₂Cl₂ (4 mL) was added to the reaction mixture. The mixture was stirred for 18 h at room temperature and then poured into ice water, and ex-

tracted with CH₂Cl₂. The combined organic layers were dried over MgSO₄ and filtered. The filtrate was dried under vacuum, and the crude product was further purified by column chromatography on silica gel with hexanes/CH₂Cl₂ (6:1 v/v) as the eluent. The product was obtained as a colorless oil (2.2 g, 99%). ¹H NMR (CDCl₃, 400 MHz): δ = 7.23 (d, 2H, *J* = 8.4 Hz), 7.09 (d, 2H, *J* = 8.8 Hz), 7.06 (d, 1H, *J* = 2.0 Hz), 6.93 (dd, 1H, *J* = 7.2, 1.6 Hz), 6.87 (dd, 1H, *J* = 7.2, 1.6 Hz), 6.81–6.76 (m, 2H), 6.14 (dd, 1H, *J* = 7.6, 0.8 Hz), 5.99 (d, 1H, *J* = 8.8 Hz), 4.01 (t, 2H, *J* = 6.0 Hz), 1.84–1.79 (m, 2H), 1.49–1.47 (m, 2H), 1.36 (m, 4H), 0.91 ppm (t, 3H, *J* = 5.0 Hz).

10-(4-{2-[2-(2-Methoxyethoxy)ethoxy]ethoxy}phenyl)-10H-phenothiazine-3-carbaldehyde (5)

Compound **1** (1.54 g, 3.52 mmol) was added to a 100 mL round-bottomed flask and dry DMF (4 mL) was injected under nitrogen at 0 °C. POCl₃ (0.38 mL, 4.06 mmol) was injected slowly into the solution, which was stirred for 1 h. The mixture was heated at 60 °C for 20 h. The mixture was extracted with CH₂Cl₂, and the organic extracts were collected and dried over MgSO₄. After filtration, the filtrate was dried under vacuum. The crude product was further purified by column chromatography with CH₂Cl₂/EA (10:1 v/v) as the eluent. The product was obtained as a yellow solid (0.80 g, 52%). ¹H NMR ([D₆]acetone, 400 MHz): δ = 9.74 (s, 1H), 7.48 (d, 1H, *J* = 1.6 Hz), 7.42 (dd, 1H, *J* = 8.4, 2.0 Hz), 7.38 (d, 2H, *J* = 8.8 Hz), 7.28 (d, 2H, *J* = 8.8 Hz), 7.02 (dd, 1H, *J* = 7.2, 2.0 Hz), 6.95–6.87 (m, 2H), 6.29 (d, 1H, *J* = 8.8 Hz), 6.21 (dd, 1H, *J* = 8.0, 1.6 Hz), 4.27 (t, 2H, *J* = 4.8 Hz), 3.89 (t, 2H, *J* = 4.8 Hz), 3.71–3.68 (m, 2H), 3.64–3.59 (m, 4H), 3.49–3.47 (m, 2H), 3.29 ppm (s, 3H).

3-[4-(Hexyloxy)phenyl]-10-(4-{2-[2-(2-methoxyethoxy)ethoxy]ethoxy}phenyl)-10H-phenothiazine (6)

Compound **3** (1.50 g, 2.90 mmol), tributyl[4-(hexyloxy)phenyl]stannane (2.00 g, 4.28 mmol), and [PdCl₂(PPh₃)₂] (0.10 g, 5 mol%) as the catalyst were added under nitrogen to a 50 mL round-bottomed flask. Dry DMF (3 mL) was injected into the mixture, which was heated at 100 °C for 18 h. After cooling, the mixture was quenched with an aqueous solution of KF and the aqueous layer was extracted with CH₂Cl₂. The combined organic layers were dried over MgSO₄ and evaporated to dryness. The crude product was further purified by column chromatography on silica gel with CH₂Cl₂/EA (50:1 v/v) as the eluent. The product was obtained as a colorless oil (0.4 g, 22%). ¹H NMR ([D₆]acetone, 400 MHz): δ = 7.48 (d, 2H, *J* = 8.4 Hz), 7.36 (d, 2H, *J* = 8.8 Hz), 7.26 (d, 2H, *J* = 8.8 Hz), 7.24 (s, 1H), 7.13 (dd, 1H, *J* = 8.8, 2.0 Hz), 7.02 (dd, 1H, *J* = 7.6, 2.0 Hz), 6.95 (d, 2H, *J* = 8.4 Hz), 6.92–6.88 (m, 1H), 6.84–6.80 (m, 1H), 6.25 (d, 1H, *J* = 8.4 Hz), 6.22 (d, 1H, *J* = 8.0 Hz), 4.26 (t, 2H, *J* = 4.8 Hz), 4.01 (t, 2H, *J* = 6.4 Hz), 3.89 (d, 2H, *J* = 4.8 Hz), 3.71–3.68 (m, 2H), 3.64–3.59 (m, 4H), 3.50–3.47 (m, 2H), 3.30 (s, 3H), 1.80–1.73 (m, 2H), 1.50–1.44 (m, 2H), 1.36–1.31 (m, 4H), 0.90 ppm (t, 3H, *J* = 5.6 Hz).

10-[4-(Hexyloxy)phenyl]-3-(4-{2-[2-(2-methoxyethoxy)ethoxy]ethoxy}phenyl)-10H-phenothiazine (7)

Compound **4** (0.80 g, 1.76 mmol), tributyl[4-(2-[2-(2-methoxyethoxy)ethoxy]ethoxy)phenyl]stannane (1.2 g, 2.27 mmol), and [PdCl₂(PPh₃)₂] (0.040 g, 5 mol%) as the catalyst were added to a 50 mL round-bottomed flask under nitrogen. Dry DMF (3.0 mL) was injected into the mixture, which was heated at 100 °C for 18 h. After cooling, the mixture was quenched with an aqueous solution of KF and the aqueous layer was extracted with CH₂Cl₂. The combined organic layers were dried over MgSO₄ and filtered. The filtrate was evaporated to dryness, and the crude product was further purified by column chromatography on silica gel with CH₂Cl₂/

EA (50:1 *v/v*) as the eluent. The product was obtained as a colorless oil (0.50 g, 65%). ¹H NMR ([D₆]acetone, 400 MHz): δ = 7.49 (d, 2H, *J* = 8.4 Hz), 7.35 (d, 2H, *J* = 8.8 Hz), 7.25 (d, 2H, *J* = 8.8 Hz), 7.24 (s, 1H), 7.14 (dd, 1H, *J* = 8.8, 2.0 Hz), 7.02 (dd, 1H, *J* = 7.6, 2.0 Hz), 6.99 (d, 2H, *J* = 8.4 Hz), 6.95–6.91 (m, 1H), 6.88–6.80 (m, 1H), 6.25 (d, 1H, *J* = 8.4 Hz), 6.22 (d, 1H, *J* = 8.0 Hz), 4.26 (t, 2H, *J* = 4.8 Hz), 4.01 (t, 2H, *J* = 6.4 Hz), 3.89 (d, 2H, *J* = 4.8 Hz), 3.71–3.68 (m, 2H), 3.64–3.59 (m, 4H), 3.50–3.47 (m, 2H), 3.30 (s, 3H), 1.80–1.73 (m, 2H), 1.50–1.44 (m, 2H), 1.36–1.31 (m, 4H), 0.90 ppm (t, 3H, *J* = 5.6 Hz).

3,10-Bis[4-(hexyloxy)phenyl]-10*H*-phenothiazine (8)

Compound **4** (0.48 g, 1.06 mmol), tributyl[4-(hexyloxy)phenyl]stannane (0.6 g, 1.28 mmol), and [PdCl₂(PPh₃)₂] (0.040 g, 5 mol%) as the catalyst were added to a 50 mL round-bottomed flask under nitrogen. Dry DMF (3 mL) was injected into the mixture, which was heated at 100 °C for 18 h. After cooling, the mixture was quenched with an aqueous solution of KF and the aqueous layer was extracted with CH₂Cl₂. The combined organic layers were dried over MgSO₄ and filtered. The filtrate was evaporated to dryness, and the crude product was further purified by column chromatography on silica gel with hexanes/CH₂Cl₂ (6:1 *v/v*) as the eluent. The product was obtained as a colorless oil (0.2 g, 34%). ¹H NMR ([D₆]acetone, 400 MHz): δ = 7.48 (d, 2H, *J* = 8.4 Hz), 7.35 (d, 2H, *J* = 8.8 Hz), 7.24 (d, 2H, *J* = 8.8 Hz), 7.22 (s, 1H), 7.13 (dd, 1H, *J* = 8.4, 2.0 Hz), 7.02 (dd, 1H, *J* = 7.6, 2.0 Hz), 6.95 (d, 2H, *J* = 8.4 Hz), 6.90–6.88 (m, 1H), 6.84–6.80 (m, 1H), 6.24 (d, 1H, *J* = 8.4 Hz), 6.22 (dd, 1H, *J* = 8.4, 1.2 Hz), 4.11 (t, 2H, *J* = 6.4 Hz), 4.01 (t, 2H, *J* = 6.4 Hz), 1.88–1.81 (m, 2H), 1.80–1.73 (m, 2H), 1.54–1.44 (m, 4H), 1.40–1.33 (m, 8H), 0.94 ppm (t, 6H, *J* = 5.2 Hz).

7-Bromo-10-[4-(hexyloxy)phenyl]-10*H*-phenothiazine-3-carbaldehyde (9)

Compound **5** was dissolved in CH₂Cl₂ (2 mL) in a round-bottomed flask and a solution of NBS (0.53 g, 2.98 mmol) in CH₂Cl₂ (2 mL) was added to the reaction mixture. The mixture was stirred for 18 h at room temperature and then poured into ice water, and extracted with CH₂Cl₂. The combined organic layers were dried over MgSO₄ and filtered. The filtrate was evaporated to dryness, and the crude product was further purified by column chromatography on silica gel with hexanes/CH₂Cl₂ (6:1 *v/v*) as the eluent. The product was obtained as a yellow oil (1.3 g, 99%). ¹H NMR ([D₆]acetone, 400 MHz): δ = 9.75 (s, 1H), 7.69 (d, 1H, *J* = 1.6 Hz), 7.45 (dd, 1H, *J* = 8.4, 1.6 Hz), 7.38 (d, 2H, *J* = 8.8 Hz), 7.28 (d, 2H, *J* = 8.8 Hz), 7.19 (d, 1H, *J* = 2.0 Hz), 7.07 (dd, 1H, *J* = 8.8, 2.0 Hz), 6.30 (d, 1H, *J* = 8.8 Hz), 6.12 (d, 1H, *J* = 8.8 Hz), 4.01 (t, 2H, *J* = 6.0 Hz), 1.84–1.79 (m, 2H), 1.49–1.47 (m, 2H), 1.36 (m, 4H), 0.91 ppm (t, 3H, *J* = 5.0 Hz).

7-[4-(Hexyloxy)phenyl]-10-(4-{2-[2-(2-methoxyethoxy)ethoxy]phenyl})-10*H*-phenothiazine-3-carbaldehyde (EO1 a)

Compound **6** (0.40 g, 0.65 mmol) was added to a 100 mL round-bottomed flask and dry DMF (2 mL) was injected under nitrogen at 0 °C. POCl₃ (0.3 mL, 3.25 mmol) was injected slowly into the solution, which was stirred for 1 h. The mixture was heated at 65 °C for 20 h. The mixture was extracted with CH₂Cl₂, and the organic extracts were collected and dried over MgSO₄. After filtration, the filtrate was dried under vacuum. The crude product was further purified by column chromatography with CH₂Cl₂/EA (6:1 *v/v*) as the eluent. The product was obtained as a yellow oil (0.3 g, 75%). ¹H NMR ([D₆]acetone, 400 MHz): δ = 9.74 (s, 1H), 7.50 (d, 2H, *J* =

8.8 Hz), 7.49 (s, 1H), 7.42 (d, 1H, *J* = 8.4 Hz), 7.39 (d, 2H, *J* = 8.8 Hz), 7.28 (d, 2H, *J* = 8.8 Hz), 7.26 (dd, 1H, *J* = 7.2, 2.0 Hz), 7.15 (dd, 1H, *J* = 8.8, 2.0 Hz), 6.96 (d, 2H, *J* = 8.4 Hz), 6.28 (d, 1H, *J* = 8.4 Hz), 6.23 (d, 1H, *J* = 8.4 Hz), 4.27 (t, 1H, *J* = 4.0 Hz), 4.01 (t, 2H, *J* = 6.4 Hz), 3.89 (t, 2H, *J* = 4.4 Hz), 3.70 (t, 2H, *J* = 4.0 Hz), 3.64–3.59 (m, 4H), 3.48 (t, 2H, *J* = 4.4 Hz), 3.30 (s, 3H), 1.77 (m, 2H), 1.47 (m, 2H), 1.35 (m, 4H), 0.90 ppm (t, 3H, *J* = 6.8 Hz); HRMS (FAB): *m/z* calcd for C₃₈H₄₃NO₆S [M]⁺: 641.2811; found: 641.2806.

(E)-2-Cyano-3-[7-(4-(hexyloxy)phenyl)-10-(4-{2-[2-(2-methoxyethoxy)ethoxy]ethoxy}phenyl)-10*H*-phenothiazin-3-yl)acrylic acid (EO1)

Sensitizer EO1a (0.10 g, 0.16 mmol), cyanoacetic acid (0.05 g, 0.32 mmol), and NH₄OAc (2.97 mg) were added to a 100 mL round-bottomed flask. AcOH (2 mL) was added to the mixture, which was heated at 110 °C for 20 h. After the solution was cooled to room temperature, the volatile compounds were removed in vacuo, and the residue was extracted with EA. The organic extracts were collected and dried over MgSO₄. After filtration, the filtrate was dried under vacuum. The crude product was further purified by column chromatography on silica gel with CH₂Cl₂/EA (1:1 *v/v*) as the eluent. The product was obtained as a red solid (80 mg, 73%). ¹H NMR ([D₆]acetone, 400 MHz): δ = 8.06 (s, 1H), 7.81 (s, 1H), 7.62 (d, 1H, *J* = 8.8 Hz), 7.51 (d, 2H, *J* = 8.4 Hz), 7.42 (d, 2H, *J* = 8.8 Hz), 7.30 (d, 2H, *J* = 8.8 Hz), 7.28 (d, 1H, *J* = 2.0 Hz), 7.17 (dd, 1H, *J* = 8.8, 1.6 Hz), 6.97 (d, 1H, *J* = 8.8 Hz), 6.27 (d, 1H, *J* = 8.8 Hz), 6.24 (d, 1H, *J* = 8.8 Hz), 4.28 (t, 2H, *J* = 4.8 Hz), 4.02 (t, 2H, *J* = 6.4 Hz), 3.90 (t, 2H, *J* = 4.8 Hz), 3.70 (dd, 2H, *J* = 5.2, 4.0 Hz), 3.64–3.59 (m, 4H), 3.49 (dd, 2H, *J* = 5.2, 4.4 Hz), 3.30 (s, 3H), 1.81–1.74 (m, 2H), 1.50–1.44 (m, 2H), 1.39–1.34 (m, 4H), 0.90 ppm (t, 3H, *J* = 6.8 Hz); ¹³C NMR ([D₆]acetone, 500 MHz): δ = 164.3, 160.5, 160.0, 153.3, 149.1, 142.3, 137.4, 133.2, 132.6, 132.4, 129.3, 128.2, 127.0, 126.1, 125.1, 120.6, 120.2, 118.1, 118.0, 117.3, 116.4, 115.9, 72.8, 71.6, 71.5, 71.3, 70.5, 69.1, 68.8, 32.4, 26.6, 23.4, 14.4 ppm; HRMS (FAB): *m/z* calcd for C₄₁H₄₄N₂O₇S [M]⁺: 708.2863; found: 708.2856; elemental analysis calcd (%) for C₄₁H₄₄N₂O₇S: C 69.47, H 6.26, N 3.95; found: C 69.23, H 6.15, N 4.20.

10-[4-(Hexyloxy)phenyl]-7-(4-{2-[2-(2-methoxyethoxy)ethoxy]ethoxy}phenyl)-10*H*-phenothiazine-3-carbaldehyde (EO2 a)

Compound **7** (0.53 g, 0.96 mmol) was added to a 100 mL round-bottomed flask and dry DMF (3.0 mL) was injected under nitrogen at 0 °C. POCl₃ (0.16 mL, 1.92 mmol) was injected slowly into the solution, which was stirred for 1 h and then heated at 65 °C for 20 h. The mixture was extracted with CH₂Cl₂, and the organic extracts were collected and dried over MgSO₄. After filtration, the filtrate was dried under vacuum. The crude product was further purified by column chromatography with CH₂Cl₂/EA (6:1 *v/v*) as the eluent. The product was obtained as a yellow solid (0.14 g, 25%). ¹H NMR ([D₆]acetone, 400 MHz): δ = 9.74 (s, 1H), 7.51 (d, 2H, *J* = 8.8 Hz), 7.50 (s, 1H), 7.42 (d, 1H, *J* = 8.4 Hz), 7.41 (d, 2H, *J* = 8.8 Hz), 7.27 (d, 2H, *J* = 8.8 Hz), 7.26 (dd, 1H, *J* = 7.2, 2.0 Hz), 7.15 (dd, 1H, *J* = 8.8, 2.0 Hz), 6.99 (d, 2H, *J* = 8.4 Hz), 6.28 (d, 1H, *J* = 8.4 Hz), 6.24 (d, 1H, *J* = 8.4 Hz), 4.27 (t, 1H, *J* = 4.0 Hz), 4.01 (t, 2H, *J* = 6.4 Hz), 3.89 (t, 2H, *J* = 4.4 Hz), 3.70 (t, 2H, *J* = 4.0 Hz), 3.64–3.59 (m, 4H), 3.48 (t, 2H, *J* = 4.4 Hz), 3.30 (s, 3H), 1.77 (m, 2H), 1.47 (m, 2H), 1.35 (m, 4H), 0.90 ppm (t, 3H, *J* = 6.8 Hz); HRMS (FAB): *m/z* calcd for C₃₈H₄₃NO₆S [M]⁺: 641.2811; found: 641.2820.

(E)-3-[7-[4-(2,5,7,9-Tetraoxaundecan-11-yl)phenyl]-10-[4-(hexyloxy)phenyl]-10H-phenothiazin-3-yl]-2-cyanoacrylic acid (EO2)

Sensitizer EO2a (0.14 g, 0.16 mmol), cyanoacetic acid (0.05 g, 0.32 mmol), and NH₄OAc (2.97 mg) were added to a 100 mL round-bottomed flask. AcOH (2 mL) was added as the solvent, and the solution was heated at 110 °C for 20 h. After the solution was cooled to room temperature, the volatile compounds were removed in vacuo, and the residue was extracted with EA. The organic extracts were collected and dried over MgSO₄. After filtration, the filtrate was dried under vacuum. The crude product was further purified by column chromatography on silica gel with CH₂Cl₂/EA (1:1 v/v) as the eluent. The product was obtained as a red solid (80 mg, 73%). ¹H NMR ([D₆]acetone, 400 MHz): δ = 8.06 (s, 1H), 7.81 (d, 1H, J = 1.6 Hz), 7.62 (dd, 1H, J = 8.8, 2.0 Hz), 7.52 (d, 2H, J = 8.8 Hz), 7.40 (d, 2H, J = 8.8 Hz), 7.27 (d, 2H, J = 8.8 Hz), 7.26 (d, 1H, J = 2.4 Hz), 7.17 (dd, 1H, J = 8.8, 2.4 Hz), 6.99 (d, 1H, J = 8.8 Hz), 6.27 (d, 1H, J = 8.8 Hz), 6.24 (d, 1H, J = 8.8 Hz), 4.28 (t, 2H, J = 4.8 Hz), 4.02 (t, 2H, J = 6.4 Hz), 3.90 (t, 2H, J = 4.8 Hz), 3.70 (dd, 2H, J = 5.2, 4.0 Hz), 3.64–3.59 (m, 4H), 3.49 (dd, 2H, J = 5.2, 4.4 Hz), 3.30 (s, 3H), 1.81–1.74 (m, 2H), 1.50–1.44 (m, 2H), 1.39–1.34 (m, 4H), 0.90 ppm (t, 3H, J = 6.8 Hz); ¹³C NMR ([D₆]acetone, 500 MHz): δ = 164.7, 161.0, 160.2, 153.7, 149.6, 142.7, 137.7, 133.3, 133.1, 133.0, 129.8, 128.7, 127.4, 126.5, 125.5, 121.0, 120.5, 118.4, 117.7, 116.8, 116.4, 110.7, 73.2, 72.0, 71.8, 71.7, 70.9, 69.6, 69.0, 59.3, 32.9, 29.9, 27.0, 23.9, 14.9 ppm; HRMS (FAB): *m/z* calcd for C₄₁H₄₄N₂O₇S [M]⁺: 708.2864; found: 708.2853; elemental analysis calcd (%) for C₄₁H₄₄N₂O₇S: C 69.47, H 6.26, N 3.95; found: C 69.52, H 6.57, N 3.71.

7-[4-(2,5,7,9-Tetraoxaundecan-11-yl)phenyl]-10-[4-[2-(2-methoxyethoxy)ethylperoxy]phenyl]-10H-phenothiazine-3-carbaldehyde (EO3a)

10-[4-(hexyloxy)phenyl]-7-(4,4,5,5-tetramethyl-1,3,2-dioxaborolan-2-yl)-10H-phenothiazine-3-carbaldehyde (1.09 g, 1.86 mmol), 1-bromo-4-[2-[2-(2-methoxyethoxy)ethoxy]ethoxy]benzene (0.89 g, 1.86 mmol), potassium carbonate (1.54 g, 11.16 mmol), and [Pd(PPh₃)₄] (0.11 g) were added to a 100 mL two-necked round-bottomed flask under nitrogen. Dry toluene (3 mL) and water (3 mL) were injected into the flask. The mixture was heated at 120 °C for 20 h. The mixture was extracted with CH₂Cl₂ and washed with brine. The organic extracts collected were dried over MgSO₄. The crude product was further purified by column chromatography with CH₂Cl₂/EA (4:1 v/v) as the eluent. The product was obtained as a yellow solid (0.57 g, 44%). ¹H NMR (CDCl₃, 400 MHz): δ = 9.68 (s, 1H), 7.44 (d, 1H, J = 2.0 Hz), 7.36 (d, 2H, J = 8.8 Hz), 7.27 (d, 2H, J = 8.8 Hz), 7.26 (dd, 1H, J = 8.8, 2.0 Hz), 7.15 (d, 2H, J = 8.8 Hz), 7.12 (d, 1H, J = 2.0 Hz), 6.97 (dd, 1H, J = 8.8, 2.0 Hz), 6.92 (d, 2H, J = 8.8 Hz), 6.17 (d, 1H, J = 8.0 Hz), 6.15 (d, 1H, J = 8.0 Hz), 4.28 (t, 2H, J = 4.4 Hz), 4.15 (t, 2H, J = 4.4 Hz), 3.90 (t, 2H, J = 4.8 Hz), 3.82 (t, 2H, J = 4.8 Hz), 3.70–3.58 (m, 12H), 3.50–3.45 (m, 4H), 3.29 (s, 3H), 3.27 ppm (s, 3H); HRMS (FAB): *m/z* calcd for C₃₉H₄₅NO₅S [M]⁺: 703.2810; found: 703.2807.

(E)-3-[7-[4-(2,5,7,9-Tetraoxaundecan-11-yl)phenyl]-10-[4-[2-(2-methoxyethoxy)ethylperoxy]phenyl]-10H-phenothiazin-3-yl]-2-cyanoacrylic acid (EO3)

Sensitizer EO3a (0.30 g, 0.43 mmol), cyanoacetic acid (0.08 g, 0.94 mmol), and NH₄OAc (2.97 mg) were added to a 100 mL round-bottomed flask. AcOH (2 mL) was added as the solvent, and the so-

lution was heated at 110 °C for 20 h. After the solution was cooled to room temperature, the volatile compounds were removed in vacuo, and the residue was extracted with EA. The organic extracts were collected and dried over MgSO₄. After filtration, the filtrate was dried under vacuum. The crude product was further purified by column chromatography on silica gel with EA as the eluent. The product was obtained as a red solid (0.17 g, 47%). ¹H NMR ([D₆]acetone, 400 MHz): δ = 8.07 (s, 1H), 7.81 (d, 1H, J = 2.0 Hz), 7.63 (dd, 1H, J = 8.8, 2.0 Hz), 7.52 (d, 2H, J = 8.8 Hz), 7.42 (d, 2H, J = 8.8 Hz), 7.30 (d, 2H, J = 8.8 Hz), 7.29 (d, 1H, J = 2.0 Hz), 7.17 (dd, 1H, J = 8.8, 2.0 Hz), 6.99 (d, 2H, J = 8.8 Hz), 6.27 (d, 1H, J = 8.4 Hz), 6.24 (d, 1H, J = 8.4 Hz), 4.28 (t, 2H, J = 4.4 Hz), 4.15 (t, 2H, J = 4.4 Hz), 3.90 (t, 2H, J = 4.8 Hz), 3.82 (t, 2H, J = 4.8 Hz), 3.70–3.58 (m, 12H), 3.50–3.45 (m, 4H), 3.29 (s, 3H), 3.27 ppm (s, 3H); ¹³C NMR ([D₆]acetone, 500 MHz): δ = 164.7, 160.6, 160.0, 153.6, 149.3, 142.5, 137.4, 133.3, 132.9, 132.8, 129.7, 128.5, 127.2, 126.4, 125.4, 120.8, 120.4, 118.27, 118.2, 117.7, 116.6, 116.2, 110.6, 73.08, 73.05, 71.9, 71.8, 71.70, 71.66, 71.52, 71.50, 70.74, 70.69, 69.2, 68.8, 59.23, 59.21 ppm; HRMS (FAB): *m/z* calcd for C₄₂H₄₆N₂O₁₀S [M]⁺: 770.2868; found: 770.2861; elemental analysis calcd (%) for C₄₂H₄₆N₂O₁₀S: C 65.44, H 6.01, N 3.63; found: C 65.31, H 5.92, N 3.69.

7-(2,4-Bis[2-[2-(2-methoxyethoxy)ethoxy]ethoxy]phenyl)-10-[4-[2-(2-methoxyethoxy)ethylperoxy]phenyl]-10H-phenothiazine-3-carbaldehyde (EO4a)

10-[4-[2-(2-methoxyethoxy)ethylperoxy]phenyl]-7-(4,4,5,5-tetramethyl-1,3,2-dioxaborolan-2-yl)-10H-phenothiazine-3-carbaldehyde (0.57 g, 0.96 mmol), 1-bromo-2,4-bis[2-[2-(2-methoxyethoxy)ethoxy]ethoxy]benzene (0.55 g, 1.14 mmol), potassium carbonate (0.90 g, 6.51 mmol), and [Pd(PPh₃)₄] (0.060 g) were added to a 100 mL two-necked round-bottomed flask under nitrogen. Dry toluene (2.0 mL) and water (2.0 mL) were injected into the flask, and the solution was heated at 120 °C for 20 h. The mixture was extracted with CH₂Cl₂ and washed with brine. The collected organic extracts were dried over MgSO₄ and filtered. The filtrate was dried under vacuum, and the crude product was further purified by column chromatography with EA/MeOH (20:1 by v/v) as the eluent. The product was obtained as a yellow oil (0.12 g, 15%). ¹H NMR ([D₆]acetone, 400 MHz): δ = 9.74 (s, 1H), 7.49 (d, 1H, J = 2.0 Hz), 7.43 (dd, 1H, J = 8.8, 2.0 Hz), 7.41 (d, 2H, J = 8.8 Hz), 7.31 (d, 2H, J = 8.8 Hz), 7.30 (d, 1H, J = 2.0 Hz), 7.21 (d, 1H, J = 8.4 Hz), 7.12 (dd, 1H, J = 8.8, 2.0 Hz), 6.67 (d, 1H, J = 2.0 Hz), 6.59 (dd, 1H, J = 8.4, 2.0 Hz), 6.29 (d, 1H, J = 8.8 Hz), 6.21 (d, 1H, J = 8.8 Hz), 4.28 (t, 2H, J = 4.8 Hz), 4.16 (t, 4H, J = 4.8 Hz), 3.90 (t, 2H, J = 4.8 Hz), 3.83–3.78 (m, 4H), 3.70 (t, 2H, J = 4.8 Hz), 3.65–3.57 (m, 14H), 3.54–3.41 (m, 8H), 3.29 (s, 3H), 3.28 (s, 3H), 3.25 ppm (s, 3H); HRMS (FAB): *m/z* calcd for C₄₆H₅₉NO₁₃S [M]⁺: 865.3702; found: 865.3707.

(E)-3-[7-(2,4-Bis[2-[2-(2-methoxyethoxy)ethoxy]ethoxy]phenyl)-10-[4-[2-(2-methoxyethoxy)ethylperoxy]phenyl]-10H-phenothiazin-3-yl]-2-cyanoacrylic acid (EO4)

Sensitizer EO4a (0.12 g, 0.14 mmol), cyanoacetic acid (0.060 g, 0.71 mmol), and NH₄OAc (2.97 mg) were added to a 100 mL round-bottomed flask. AcOH (2.0 mL) was added as the solvent, and the solution was heated at 110 °C for 20 h. After the solution was cooled to room temperature, the volatile compounds were removed in vacuo, and the residue was extracted with EA. The organic extracts were collected and dried over MgSO₄. After filtration, the filtrate was dried under vacuum. The crude product was further purified by column chromatography on silica gel with EA as

the eluent. The product was obtained as a red solid (0.12 g, 28%). ¹H NMR (CDCl₃, 400 MHz): δ = 7.89 (s, 1H), 7.51 (s, 1H), 7.44 (d, 1H, *J* = 8.8 Hz), 7.23 (d, 2H, *J* = 8.8 Hz), 7.14 (d, 2H, *J* = 8.8 Hz), 7.13 (s, 1H), 7.10 (d, 1H, *J* = 8.0 Hz), 6.94 (d, 1H, *J* = 8.8 Hz), 6.51 (s, 1H), 6.49 (d, 1H, *J* = 8.8 Hz), 6.10 (d, 1H, *J* = 8.8 Hz), 6.08 (d, 1H, *J* = 8.8 Hz), 4.19 (t, 2H, *J* = 4.8 Hz), 4.11 (t, 2H, *J* = 4.8 Hz), 4.06 (t, 2H, *J* = 4.8 Hz), 3.90 (t, 2H, *J* = 4.8 Hz), 3.83 (t, 2H, *J* = 4.8 Hz), 3.77–3.63 (m, 20H), 3.60–3.43 (m, 6H), 3.37 (s, 3H), 3.35 (s, 3H), 3.32 ppm (s, 3H); ¹³C NMR (CDCl₃, 500 MHz): δ = 166.1, 159.4, 159.0, 156.5, 153.6, 148.7, 140.5, 134.8, 132.1, 131.6, 131.5, 130.4, 129.2, 127.9, 127.5, 125.3, 122.0, 120.1, 118.0, 117.0, 116.3, 116.1, 115.2, 106.0, 100.8, 97.4, 71.93, 71.90, 71.9, 70.9, 70.8, 70.71, 70.68, 70.63, 70.56, 70.53, 70.47, 69.7, 69.6, 69.5, 68.0, 67.8, 67.5, 59.0, 59.02, 58.98 ppm; HRMS (FAB): *m/z* calcd for C₄₉H₆₀N₂O₄S [M]⁺: 932.3760; found: 932.3754; elemental analysis calcd (%) for C₄₉H₆₀N₂O₄S: C 63.07, H 6.48, N 3.00; found: C 63.12, H 6.51, N 2.78.

7,10-Bis[4-(hexyloxy)phenyl]-10H-phenothiazine-3-carbaldehyde (EO5 a)

Compound **8** (0.20 g, 0.36 mmol) was added to a 100 mL round-bottomed flask and dry DMF (2.0 mL) was injected as the solvent under nitrogen at 0 °C. POCl₃ (0.10 mL, 1.08 mmol) was injected slowly into the solution, which was stirred for 1 h, and the mixture was heated at 65 °C for 20 h. The mixture was extracted with CH₂Cl₂, and the organic extracts were collected and dried over MgSO₄. After filtration, the filtrate was dried under vacuum. The crude product was further purified by column chromatography with hexanes/CH₂Cl₂ (1:1 v/v) as the eluent. The product was obtained as a yellow oil (70 mg, 33%). ¹H NMR ([D₂]acetone, 400 MHz): δ = 9.67 (s, 1H), 7.44 (d, 1H, *J* = 2.0 Hz), 7.35 (d, 2H, *J* = 8.8 Hz), 7.27 (dd, 1H, *J* = 8.4, 2.0 Hz), 7.23 (d, 2H, *J* = 8.8 Hz), 7.12 (s, 1H), 7.11 (d, 2H, *J* = 8.8 Hz), 6.97 (dd, 1H, *J* = 8.8, 2.0 Hz), 6.89 (d, 2H, *J* = 8.8 Hz), 6.18 (d, 1H, *J* = 8.4 Hz), 6.16 (d, 1H, *J* = 8.8 Hz), 4.03 (t, 2H, *J* = 6.4 Hz), 4.95 (t, 2H, *J* = 6.4 Hz), 1.86–1.73 (m, 4H), 1.50–1.40 (m, 4H), 1.38–1.30 (m, 8H), 0.92 (t, 3H, *J* = 6.8 Hz), 0.90 ppm (t, 3H, *J* = 7.2 Hz); HRMS (FAB): *m/z* calcd for C₃₇H₄₁NO₃S [M]⁺: 579.2801; found: 579.2807.

(E)-3-[7,10-Bis[4-(hexyloxy)phenyl]-10H-phenothiazin-3-yl]-2-cyanoacrylic acid (EO5)

Sensitizer EO5a (0.070 g, 0.12 mmol), cyanoacetic acid (0.030 g, 0.46 mmol), and NH₄OAc (2.97 mg) were added to a 100 mL round-bottomed flask. AcOH (2.0 mL) was added as the solvent, and the solution was heated at 110 °C for 20 h. After the solution was cooled to room temperature, the volatile compounds were removed in vacuo, and the residue was extracted with EA. The organic extracts were collected and dried over MgSO₄. After filtration, the filtrate was dried under vacuum. The crude product was further purified by column chromatography on silica gel with EA as the eluent. The product was obtained as a red solid (50 mg, 58%). ¹H NMR ([D₂]acetone, 400 MHz): δ = 7.96 (s, 1H), 7.56 (d, 1H, *J* = 1.6 Hz), 7.51 (dd, 1H, *J* = 8.8, 1.6 Hz), 7.35 (d, 2H, *J* = 8.4 Hz), 7.24 (d, 2H, *J* = 8.4 Hz), 7.11 (d, 2H, *J* = 8.8 Hz), 7.10 (s, 1H), 6.97 (dd, 1H, *J* = 8.8, 2.0 Hz), 6.89 (d, 2H, *J* = 8.8 Hz), 6.16 (d, 1H, *J* = 8.4 Hz), 6.15 (d, 1H, *J* = 8.8 Hz), 4.03 (t, 2H, *J* = 6.4 Hz), 4.95 (t, 2H, *J* = 6.4 Hz), 1.86–1.74 (m, 4H), 1.50–1.42 (m, 4H), 1.37–1.32 (m, 8H), 0.91 (t, 3H, *J* = 6.8 Hz), 0.88 ppm (t, 3H, *J* = 7.2 Hz); ¹³C NMR (CDCl₃, 400 MHz): δ = 159.5, 158.8, 154.2, 148.9, 140.9, 136.8, 131.8, 131.7, 131.4, 129.5, 127.4, 125.3, 125.2, 124.6, 120.0, 119.3, 116.9, 116.0, 115.3, 114.9, 68.5, 68.2, 31.6, 29.7, 29.2, 25.7, 22.6, 14.0 ppm; HRMS (FAB): *m/z* calcd for C₄₀H₄₂N₂O₄S [M]⁺: 646.2859; found: 646.2858;

elemental analysis calcd (%) for C₄₀H₄₂N₂O₄S: C 74.27, H 6.54, N 4.33; found: C 74.28, H 6.57, N 4.25.

Acknowledgements

We acknowledge support from the National Taiwan University, the Academia Sinica (AC), the Ministry of Science and Technology (MST) (Taiwan), and the Instrumental Center of Institute of Chemistry (AC).

Keywords: dyes/pigments · electrochemistry · sensitizers · solar cells · synthesis design

- [1] a) S. Mathew, A. Yella, P. Gao, R. Humphry-Baker, F. E. Curchod/Basile, N. Ashari-Astani, I. Tavernelli, U. Rothlisberger, M. K. Nazeeruddin, M. Grätzel, *Nat. Chem.* **2014**, *6*, 242–247; b) C.-Y. Chen, M. Wang, J.-Y. Li, N. Pootrakulchote, L. Alibabaei, C.-h. Ngoc-le, J.-D. Decoppet, J.-H. Tsai, C. Grätzel, C.-G. Wu, S. M. Zakeeruddin, M. Grätzel, *ACS Nano* **2009**, *3*, 3103–3109; c) Z. Yao, M. Zhang, H. Wu, L. Yang, R. Li, P. Wang, *J. Am. Chem. Soc.* **2015**, *137*, 3799–3802.
- [2] a) W. Wu, J. Yang, J. Hua, J. Tang, L. Zhang, Y. Long, H. Tian, *J. Mater. Chem.* **2010**, *20*, 1772–1779; b) W.-I. Hung, Y.-Y. Liao, C.-Y. Hsu, H.-H. Chou, T.-H. Lee, W.-S. Kao, J. T. Lin, *Chem. Asian J.* **2014**, *9*, 357–366; c) H. Tian, X. Yang, R. Chen, Y. Pan, L. Li, A. Hagfeldt, L. Sun, *Chem. Commun.* **2007**, 3741–3743; d) C.-J. Yang, Y. J. Chang, M. Watanabe, Y.-S. Hon, T. J. Chow, *J. Mater. Chem.* **2012**, *22*, 4040–4049; e) A. S. Hart, K. C. Chandra Bikram, N. K. Subbaiyan, P. A. Karr, F. D'Souza, *ACS Appl. Mater. Interfaces* **2012**, *4*, 5813–5820; f) Y. Hua, S. Chang, D. Huang, X. Zhou, X. Zhu, J. Zhao, T. Chen, W.-Y. Wong, W.-K. Wong, *Chem. Mater.* **2013**, *25*, 2146–2153; g) W.-I. Hung, Y.-Y. Liao, T.-Hi Lee, Y.-C. Ting, J.-S. Ni, W.-S. Kao, J. T. Lin, T.-C. Wei, Y.-S. Yen, *Chem. Commun.* **2015**, *51*, 2152–2155.
- [3] T.-C. Chu, R. Y.-Y. Lin, C.-P. Lee, C.-Y. Hsu, P.-C. Shih, R. Lin, S.-R. Li, S.-S. Sun, J. T. Lin, R. Vittal, K.-C. Ho, *ChemSusChem* **2014**, *7*, 146–153.
- [4] a) R. Y.-Y. Lin, T.-M. Chuang, F.-L. Wu, P.-Y. Chen, T.-C. Chu, J.-S. Ni, M.-S. Fan, Y.-H. Lo, K.-C. Ho, J. T. Lin, *ChemSusChem* **2015**, *8*, 105–1153; b) T. Daeneke, Y. Uemura, N. W. Duffy, A. J. Mozer, N. Koumura, U. Bach, L. Spiccia, *Adv. Mater.* **2012**, *24*, 1222–1225; c) H. Tian, E. Gabrielsson, P. W. Lohse, N. Vlachopoulos, L. Kloo, A. Hagfeldt, L. Sun, *Energy Environ. Sci.* **2012**, *5*, 9752–9755; d) W. Xiang, F. Huang, Y.-B. Cheng, U. Bach, L. Spiccia, *Energy Environ. Sci.* **2013**, *6*, 121–127; e) C. Dong, W. Xiang, F. Huang, D. Fu, W. Huang, U. Bach, Y.-B. Cheng, X. Li, L. Spiccia, *Angew. Chem. Int. Ed.* **2014**, *53*, 6933–6937; *Angew. Chem.* **2014**, *126*, 7053–7057; f) H. Choi, B. S. Jeong, K. Do, M. J. Ju, K. Song, J. Ko, *New J. Chem.* **2013**, *37*, 329–336; g) H. Choi, J. Han, M. S. Kang, K. Song, J. Ko, *Bull. Korean Chem. Soc.* **2014**, *35*, 1433–1439; h) F. Bella, C. Gerbaldi, C. Barolo, M. Grätzel, *Chem. Soc. Rev.* **2015**, *44*, 3431–3473.
- [5] a) Y. Liu, A. Hagfeldt, X. R. Xiao, S. E. Lindquist, *Sol. Energy Mater. Sol. Cells* **1998**, *55*, 267–281; b) B. Macht, M. Turrion, A. Barkschat, P. Salvador, K. Ellmer, H. Tributsch, *Sol. Energy Mater. Sol. Cells* **2002**, *73*, 163–173; c) T. N. Murakami, H. Saito, S. Uegusa, N. Kawashima, T. Miyasaka, *Chem. Lett.* **2003**, *32*, 1154–1155; d) Y.-S. Sung, B. Yoo, M. K. Lim, S. Y. Lee, K.-J. Kim, *Electrochim. Acta* **2009**, *54*, 6286–6291; e) K. Zhu, S.-R. Jang, A. J. Frank, *Energy Environ. Sci.* **2012**, *5*, 9492–9495; f) C. Koenigsmann, T. S. Rippolles, B. J. Brennan, C. F. A. Negre, M. Koepf, A. C. Durrell, R. L. Milot, J. A. Torre, R. H. Crabtree, V. S. Batista, G. W. Brudvig, J. Bisquert, C. A. Schmuttenmaer, *Phys. Chem. Chem. Phys.* **2014**, *16*, 16629–16641; g) H. Zhang, L. Qiu, D. Xu, W. Zhang, F. Yan, *J. Mater. Chem. A* **2014**, *2*, 2221–2226; h) H.-J. Son, C. Prasittichai, J. E. Mondloch, L. Luo, J. Wu, D. W. Kim, O. K. Farha, J. T. Hupp, *J. Am. Chem. Soc.* **2013**, *135*, 11529–11532.
- [6] D. Kuang, C. Klein, H. J. Snaith, J.-E. Moser, R. Humphrey-Baker, P. Comte, S. M. Zakeeruddin, M. Grätzel, *Nano Lett.* **2006**, *6*, 769–773.
- [7] a) M. Nishiyama, T. Yamamoto, Y. Koie, *Tetrahedron Lett.* **1998**, *39*, 617–620; b) F. Hartwig, M. Kawatsura, S. I. Hauck, L. M. Shaughnessy, J. Alcazar-Roman, *J. Org. Chem.* **1999**, *64*, 5575–5580; c) A. Suzuki, *J. Organometallic Chem.* **1999**, *64*, 5575–5580.

- met. Chem.* **1999**, *576*, 147–168; d) J. K. Stille, *Angew. Chem. Int. Ed. Engl.* **1986**, *25*, 508–524; *Angew. Chem.* **1986**, *98*, 504–519.
- [8] *Annual Book of ASTM Standards, Vol. 14.04*, ASTM International, West Conshohocken, PA, **2003**, pp. G159–198.
- [9] a) Z. Ning, Y. Fu, H. Tian, *Energy Environ. Sci.* **2010**, *3*, 1170–1181; b) H. Tian, Z. Yu, A. Hagfeldt, L. Kloo, L. Sun, *J. Am. Chem. Soc.* **2011**, *133*, 9413–9422.
- [10] R. Y.-Y. Lin, T.-C. Chu, P.-W. Chen, J.-S. Ni, P.-C. Shih, Y.-C. Chen, K.-C. Ho, J. T. Lin, *ChemSusChem* **2014**, *7*, 2221–2229.

Received: April 30, 2015

Revised: May 19, 2015

Published online on June 22, 2015